v. 1, n. 1, 2021

Journal of
Engineering
Research

HIGH-SPEED PHOTOGRAPHY TECHNIQUE TO STUDY DROPLET FORMATION

Marcelo Bacci da Silva
Department of Chemical Engineering,
Federal University of The Triângulo Mineiro,
Uberaba, MG

Abstract: In this study the technique of high-speed photography was used to capture the high frequency dynamic phenomena involved in the problem of droplet generation on a spray nozzle-plate system. The instabilities that characterize jet transition were initially analyzed to validate the method of experimentation. The physical nature of droplet formation was also analyzed, and the more important physical phenomena were pointed out: the dynamic instabilities over the liquid sheet; the holes formation and the mass accumulation; the borders of the holes and liquid sheet. A quantitative study points out to the drop's distribution observed in the literature.
Keywords: Droplet generation, Experimental method, Nozzle-plate system.

INTRODUCTION

An experimental investigation of the physical mechanisms involved in the transition of a nozzle-plate system was conducted. The principle of this type of spray is commonly used for agricultural irrigation systems, for fuel emission in internal combustion engines and in fire protection systems (Majumder *et al.*, 2021; Yang *et al.*, 2018). The investigation was also important to understand the mass, momentum, and energy transfer mechanisms in disperse two-phase flows (Mccreery and Stoots, 1996).

An important number of works have been directed to this problem. The primary interest of such studies was to understand the mechanisms that increase heat and mass transporte rates to or from surfaces using impinging liquid jets (Borthakur *et al.*, 2017).

A more detailed review of drops formation mechanisms was developed by Kolev (1993). A first model for the transformation of a liquid sheet on drops was proposed by Dombrowski and Jones (1993). They supposed that the breakup of the instabilities that appears over the liquid sheet give rise to cylindrical ligaments and then to the drops. It will be show that the preponderant physical effects of the drop formation are due to other kind of instabilities.

The system is composed of an injection nozzle which projects a jet of water against a conical plate. The jet is concentric with the plate, as illustrated in Figure 1.

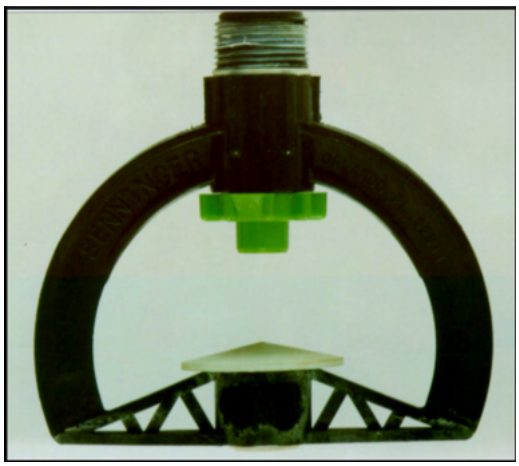

Figure 1. Spray nozzle-plate system.

A liquid sheet forms after the plate. The thickness of this sheet decreases due to radial spreading. Viscous shear forces also decrease the fluid´s momentum as it expands outward from the plate causing additional reduction in the thickness. The sheet flows in a radial direction outward from the plate, and breaks up into drops, as illustrated in Figure 2.

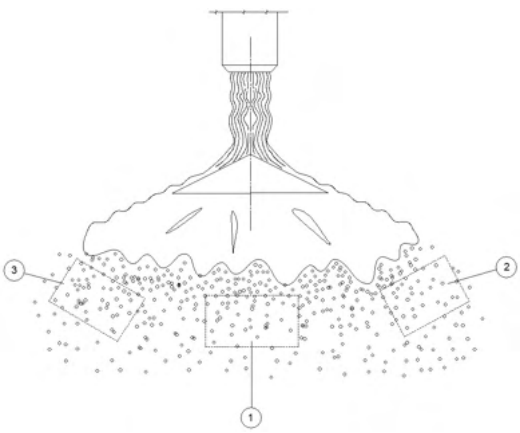

Figure 2. Spray nozzle-plate and drops position: (1) central droplets, (2) and (3) side droplets.

For a high Reynolds number, large amplitude three-dimensional waves are generated by shear forces against air. As the amplitude of the waves increase, holes are blown through the free sheet.

Drops are shed from the expanding holes. Drop size and its distribution are determined as a balance between two opposite forces: shear forces and surface tension. The first amplifies the instabilities and the second tends to hold the sheet and the drops together.

The objective of the present work was to develop a fundamental knowledge of droplet formation in spray-nozzle system and to obtain physical information to develop modern technologies for irrigation systems and other similar practical applications. These are very important concerning the reduction of water and energy consumption (Lachin *et al.*, 2020). It is also important to improve the uniformity of the irrigation area by reducing the undesirable effects of soil erosion and droplets evaporation, optimizing the agricultural production (Lachin *et al.*, 2020). This study intends to point out the physical phenomena that determine droplet formation.

A similar physical model was proposed by Chin *et al.* (1991), using a maximum entropy formalism. Yang *et al.* (2018) propose that breakup is due to the localized perforation of the liquid sheet. These phenomena were clearly pointed out in the presente study.

MODELING AND ANALYSIS

The experimental setup used to investigate the physical nature of droplet formation is show in Figure 3.

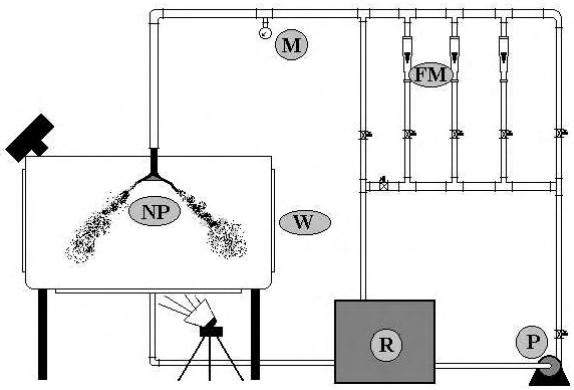

Figure 3. Sketch of the experimental apparatus.

The test section is located inside a collector chamber which is equipped with three glass windows (W). The apparatus is composed of a 2,24-kW pump (P); a water source (R); three flow meters (FM) which control the water flow; PVC piping 25 mm in diameter; an injection nozzle and a conical plate (NP). The operating pressure was monitored by a Bourdon manometer (M) located upstream the nozzle. The flow for each test was statistically steady and turbulent.

Photographs were taken using a Pentax 35mm camera and a high frequency strobe lamp, controlled by an electronic circuit to give a flash duration of four microseconds. The short-duration illumination permitted freezing high frequency phenomena like jet instabilities, waves, and perforations on the liquid sheet and drops formation. Instabilities over the jet and the free liquid sheets as well as localized perforations and mass accumulation on the borders of the liquid film were thus easily reveled by this method. A back-lighting technique, as illustrated in Figure 1 was adopted and an ISO 400 film was used.

RESULTS AND DISCUSSION

LIQUID FREE-JETS

As a preliminary investigation, a free water jet was visualized for various Reynolds numbers. This parameter is defined here as $\mathrm{Re}_d = \frac{ud}{\mathrm{n}}$, where u is the mean velocity of the

free jet, d is the nozzle diameter and v is the kinematics liquid viscosity. High speed images were obtained by the previously described technique, Figure 4.

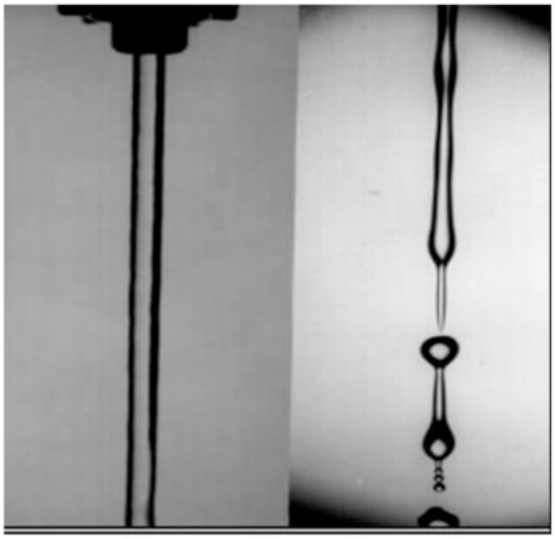

(a) (b)

Figure 4. Visualization of the Rayleigh instabilities on the free water jet, Re_d = 5,000; (a) outlet of the nozzle; (b) breakup position.

High speed images were obtained by the previously described technique. In Figure 3 it is shown that Rayleigh instabilities are developed over the free liquid jet characterized by Re_d = 5,000, and (a) shows a laminar regime in the outlet of the nozzle, while (b), in the sequence of (a), shows the breakup of the jet promoted by the Rayleigh instabilities. It is possible to see two kinds of drops: big ones that appears first with a liquid filament between them, and small ones due to Rayleigh instabilities, commonly named satellite droplets. At this low Reynolds number, the liquid surface has a very smooth appearance, without instabilities.

The flow related to a high Reynolds number, Re_d = 120,000, is shown in Figure 5. Parts (a) and (b) show the flow in a spatial sequence. Three-dimensional complex disturbance appears over the surface of the jet. They become more pronounced as the flow develops and the jet loses its regularity, with very strong periodical instabilities. They begin to inject ligaments and small droplets that characterize the beginning of the breakup. The droplets are created by an aerodynamic drag over the instabilities. These qualitative results compare very well with those of other authors: Kastengreen et al. (2017), Chigier (1991) and Mccreery and Stoots (1996).

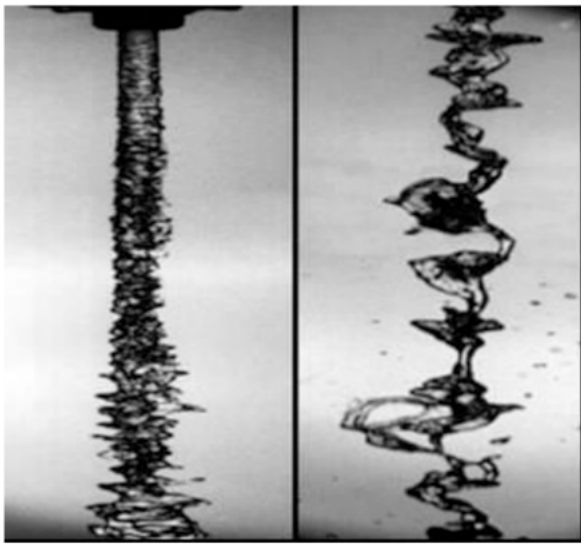

(a) (b)

Figure 5. Three dimensional instabilities on the free water jet, Re_d = 120,000; (a) outlet of the nozzle; (b) at 40 cm from the nozzle (breakup of the jet).

PHYSICAL PHENOMENA OVER THE SPRAY SYSTEM

Photographs show the overall behavior of the physical process involved in the flow transition over the spray nozzle-plate system. The turbulence structure of the jet was visualized in the last section. In this section, it is shown the flow structure over the free liquid sheet. It seems that the more important phenomena that compose this structure is the perforation that form over the sheet before the breakup and detachments of the droplets. Figure 6 shows an overall view of the flow. Sinusoidal waves are observed over the sheet which are amplified to finally degenerate into droplets.

Figure 7 shows an upper view of the liquid sheet related to Re_d = 32,000. The air shear over the sheet creates oscillations and liquid sheet thickness variations. Shear and waves result in localized high forces. When the local thickness of the sheet falls below a critical value, perforations blow in through the sheet, causing disruptions upstream the main breakup region. The sheet becomes punctured at isolated holes. These phenomena were also observed by Borthakur *et al*. (2017).

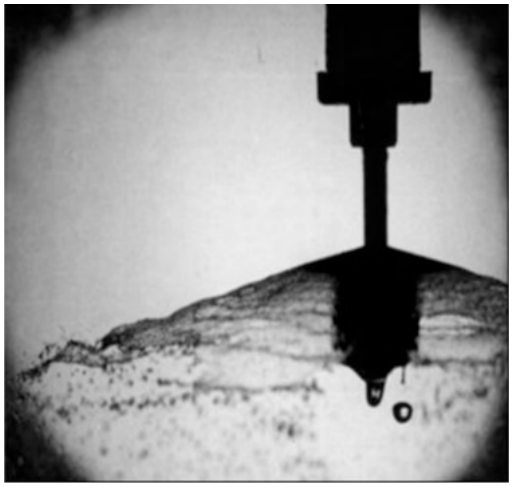

Figure 6. Overall view of the flow with sinusoidal instabilities and breakup of the liquid sheet in droplets, Re_d = 32,000; plate diameter is 44 mm and nozzle diameter is 2.8 mm.

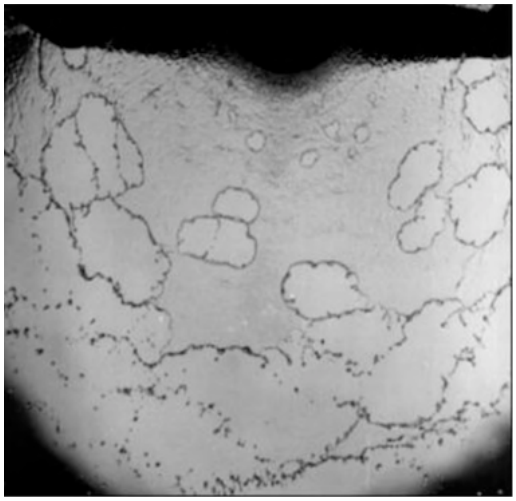

Figure 7. Upper view of the liquid sheet, with breakup into perforations and droplets, Re_d = 32,000; plate diameter is 44 mm and nozzle diameter is 2.8 mm.

The holes are amplified and give rise to liquid ligaments that breakdown into droplets. The front region of droplets characterizes a non-homogeneous droplets field in contrast with the phenomena visualized with classical methods that present a mean homogeneous appearance. It is interesting to observe that droplet formation begins on the borders as soon as the holes appear.

Figures 8 and 9 show the flow related to Re_d = 36,000 and 50,000 respectively. As the Reynolds number increases, the frequency of the holes also increases. The process of droplets formation becomes highly complex. Nevertheless, the non-homogeneous nature of the frontal region of droplets formation remains.

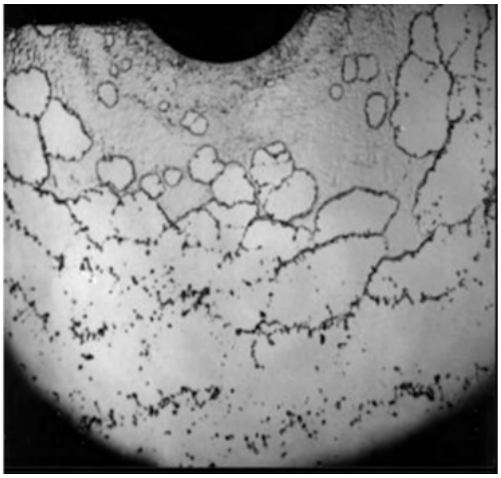

Figure 8. Upper view of the liquid sheet breakup into perforations and droplets, Re_d= 36,000; plate diameter is 44 mm and nozzle diameter is 2.8 mm.

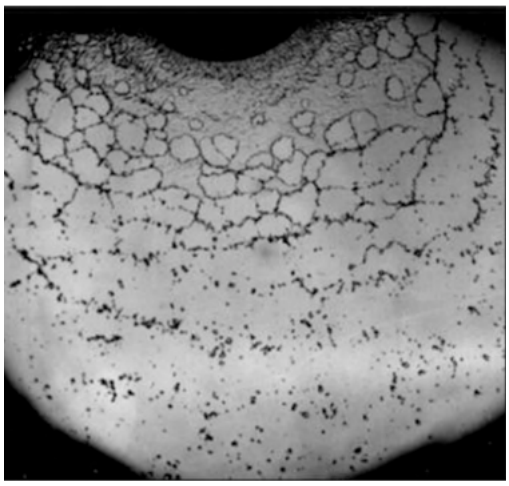

Figure 9. Upper view of the liquid sheet breakup into perforations and droplets, Re_d= 50,000; plate diameter is 44 mm and nozzle diameter is 2.8 mm.

Figure 10 shows a lateral view of the flow related to Re_d= 50,000, illustrating high amplitude oscillations. Comparing Figures 5 and 9, it is possible to see that these oscillations increase with the Reynolds number. Therefore, an increase in the Reynolds number will maximize the irrigated area. Alternatively, these oscillations can be amplified by mechanical excitation or by geometrical modifications. This is very important for practical applications, such as agricultural irrigation systems (Yang *et al.*, 2018).

Figure 10 (a), (b) and (c) show a magnified view of the front of droplets related to the flow characterized by Re_d= 32,000. Part (a) shows a magnified view of the droplet front. In the upper part of that, there is a continuous liquid film before the breakup into droplets. Part (b) is a magnified view of part (a) and clearly show the physical process of mass accumulation over the border of the sheet. Part (c) is the border of the holes. This process gives rise to localized eruptions that breakup into droplets. It seems that these eruptions are the result of surface tension gradients over the border.

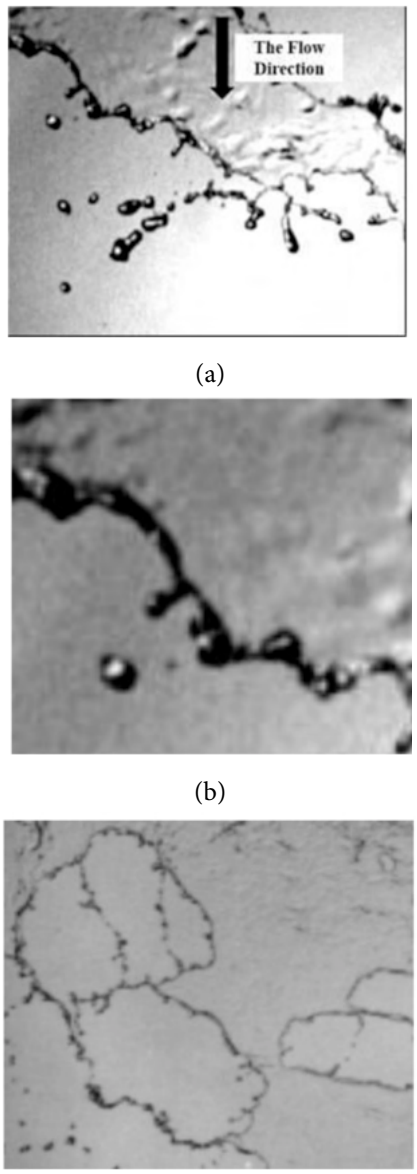

(a)

(b)

(c)

Figure 10. Magnified view of the flow related to Re_d= 32,000; plate diameter is 44 mm and nozzle diameter is 2.8 mm; (a) and (b) show the front of droplets; (c) the border of the holes.

DROPLET QUANTIFICATION

A quantitative study of high frequency phenomena, like the process of droplet formation at nozzle-plate systems, is necessary to specify the structure and geometry of droplets. This specification demands maximum precision because the quality of soil wetting is directly affected by

size, quantity, and distribution of droplets. The phenomena are captured by high-speed camera and is digitalized to permit the treatment by a software. A typical drop field is shown in Figure 11, where it is also possible to visualize a reference spherical object of 4 mm in diameter, at the left side of the Figure 11.

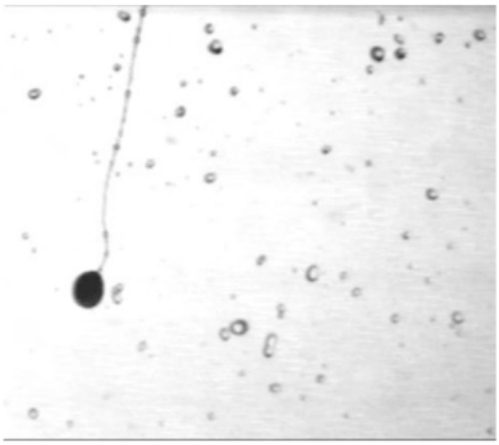

Figure 11. Overall view of a drops field to be analyzed; a reference object 4 mm in diameter is visualized on the left side of the figure.

A work area, selected over Figure 11, is shown in Figure 12. The software only works inside that limit. To quantify the droplets, the software works with the difference of gray intensity at the picture. It allows to input the maximum and minimum gray level, selecting the objects according to this range.

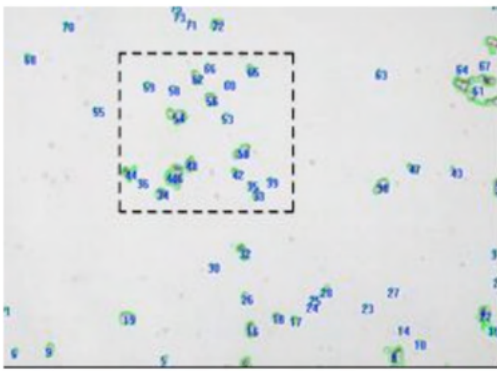

(a)

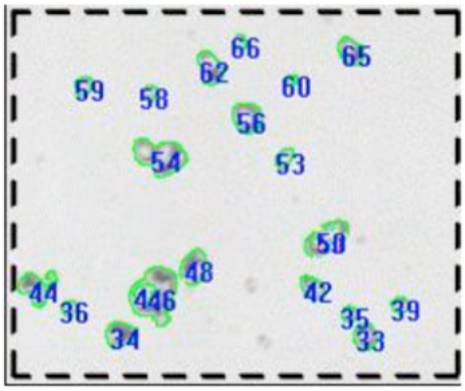

(b)

Figure 12. A selected droplets fields: (a) global view; (b) amplified droplets images.

A table of results is then obtained and transported to a software to manipulate the results and determine the droplet diameter.

To get the results in a unit system that is adequate to the applications, the software needs to be calibrated before the tests, providing a reference body with the photograph. It was used a spherical object 4 mm in diameter. As a result of this study, the distribution of the number of droplets as a function of their diameter is presented in Figure 13.

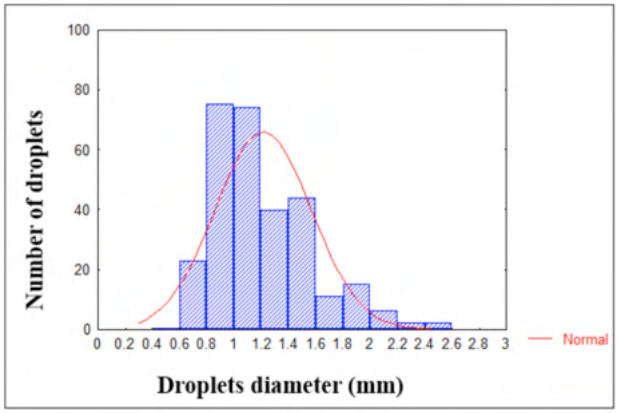

Figure 13. Droplets distribution

CONCLUSION

In this study, high speed photographic techniques were used to capture and freeze high frequency phenomena at the flow transition over a spray nozzle-plate system. The photographs show the structure of the

flow: the characteristics instabilities of the jets; the oscillations over the liquid sheet after it leaves the plate; the holes over the liquid sheet; the mass accumulation process on the border of the liquid sheet. Also visible are the ejection of droplets and ligaments of fluid in the free liquid jet. It seems that the most important physical mechanism of droplets formation pointed out is due to holes that appear over the liquid sheet. These holes are transported convectively in the radial direction and determine the non-homogeneous nature of the droplet's fronts. Another important phenomenon observed on the results, was the liquid sheet oscillations. When amplified, these oscillations give rise to a large droplet front.

REFERENCES

Borthakur, M. P.; Biswas, G.; Bandyopadhyay, D. 2017. Formation of liquids drops at an orifice and dynamics of pinch-off in liquid jets. Physical Review E 96, 013115-13211.

Chigier, N. 1991. Optical imaging of sprays. Progress in Energy and Combustion Science, 17, p. 211-262.

Chin, L. P.; Larose, P. G.; Tankin, R. S.; Jackson, T.; Sturnd, J.; Switzer, G. 1991. Droplet distributions from the breakup of a cylindrical liquid jet. Physical of Fluids A, 3, p. 1897-1906.

Dastyar, P.; Salehi, M. S.; Firoozabadi, B.; Afshin, H. 2020. Experimental investigation of the effects of surfactant on the dynamics of formation process of liquid drops. Journal of Industrial and Engineering Chemistry, 89, p. 183-193.

Kastengreen, A.; **Ilavsky, J.; Vieira, J. P.; Payri, R.; Duke, D. J.; Swantek, A.; Tilocco, F. Z.; Sovis, N.; Powell, C. F. 2017.** Measurements of droplet size in shear-driven atomization using ultra-small angle x-ray scattering. International Journal of Multiphase Flow, 92, p. 131-139.

Lachin, K.; Turchiuli, C.; Pistre, V.; Cuvelier, G.; Mezdour, S. 2020. Dimensional analysis modeling of spraying operation – impact of fluids properties and pressure nozzle geometric parameters on the pressure-flow rate relationship. Chemical Engineering Research and Design, 163, p. 36-46.

Majumder, A.; Ghosh, D.; Das, P. K. 2021. Dynamics of drop formation, growth and pinching phenomena from a submerged nozzle. Chemical Engineering Science, 245, 116808.

Mccreery, G. E.; Stoots, C. M. 1996. Drop formation mechanisms and size distributions for spray plate nozzles. International Journal of Multiphase Flow, 22, p. 431-452.

Nazari, A.; Derakhshi, A. Z.; Nazari, A.; Firoozabadi, B. 2018. Drop formation from a capillary tube: comparison of different bulk fluid on newtonian drops and formation of newtonian an non-newtonian drops in air using image processing. International Journal of Heat and Mass Transfer, 124, p. 912-919.

Yang, L.; Kapur, N.; Wang, Y.; Fiesser, F.; Bierbrauer, F.; Wilson, M. C. T.; Sabey, T.; Bain, C. D. 2018. Drop-on-demand satellite-free drop formation for precision fluid delivery. Chemical Engineering Science, 186, p.102-115.